

## Slag: What is it good for?

### Utilization of steelmaking slag to remove phosphate and neutralize acid

Nadine M. Piatak<sup>1</sup>, Robert R. Seal II<sup>1</sup>, Darryl A. Hoppe<sup>1</sup>, Carlin J. Green<sup>1</sup>, Paul M. Buszka<sup>2</sup>

<sup>1</sup>*U.S. Geological Survey, 954 National Center, Reston, Virginia, USA, npiatk@usgs.gov*

<sup>2</sup>*U.S. Geological Survey, 5957 Lakeside Blvd., Indianapolis, Indiana, USA*

**Abstract** Iron and steel slag has potential application in water treatment, beyond its current use in construction materials. Static and kinetic reactive test results using modern and legacy iron and steel slags from the Chicago-Gary area of Illinois and Indiana, USA, near Lake Michigan, demonstrated that slags are effective at removing phosphate from solutions, with modern air-cooled material being the most effective. Most slag samples additionally have high net neutralization potentials, some almost reaching that of calcite. These results indicate steelmaking slag may be a viable option for treating nutrient-rich or acidic waters.

**Key words** ferrous slag, nutrient removal, water treatment, neutralization potential, waste valorization

#### Introduction

Ferrous slag, a term that includes iron and steel slag, is the byproduct generated after smelting iron ore in a blast furnace and making steel, most commonly in a Basic Oxygen Furnace (BOF) or Electric Arc Furnace. Ferrous slag is widely used in construction but vast amounts continue to be disposed of as waste. In the Chicago-Gary area of Illinois and Indiana, USA, slag infills lake-shore wetlands and generates alkaline drainage. Regional eutrophication and local acidification are concurrent problems in waterways in these states. Utilizing locally available steelmaking slag to treat nutrient-rich or acidic waters would be a higher value alternative than the use of slag in construction, potentially offsetting restoration costs to degraded legacy areas and decreasing steel manufacturers' current waste footprint.

#### Samples and Methods

Slag from legacy sites and modern operating steelmaking facilities (tab. 1) is mostly vesicular and air-cooled, except for USSFegan, which is a granulated slag that consists of sand-sized glassy fragments. Several samples are fine grained, generally < 9.5 mm in diameter, and referred to as "C-fines." C-fines are generally the size fraction remaining after steelmakers sort air-cooled slag to recover larger fragments to sell for use in construction. Coarse composites (30 – 50 subsamples) of air-cooled slag from legacy sites were crushed to < 9.5 mm. For column experiments, two slag samples (AMFeC and ILSS5) were further crushed to < 4.75 mm to ensure adequate flow within columns (inner diameters of 5 cm and length of 23.5 cm). Samples were also sieved to > 0.5 mm to remove fines to avoid clogging. In addition to slag, commercial-grade pulverized agricultural limestone (< 2.0 mm) was used in some tests for comparison to slag.

Major elemental composition of slag was determined using wavelength dispersive X-ray fluorescence spectroscopy. The modified acid base accounting (ABA) technique was used to quantify neutralization and acid-generation potentials. Mineralogy was evaluated by X-Ray Diffraction (XRD). Particle size distribution was determined by sieving and using a hydrometer and specific surface area was measured by the Brunauer, Emmett, and Teller (BET) method.

Batch and kinetic experiments were conducted to determine phosphate removal capacities of slag. The dominant form of dissolved phosphorus (P) in this study is orthophosphate. Static batch experiments were performed on slags and limestone using end-over-end rotation and a solution to solid ratio of 1:20. Leaching solutions were prepared using deionized water and reagent-grade monopotassium phosphate ( $\text{KH}_2\text{PO}_4$ ). Based on pH, a pseudo steady state was reached after 4 days. The first set of batch experiments using 10 mg P/L reacted for 4 days, whereas the other experiments reacted for 7 days. For kinetic column experiments, the influent solution contained approximately 115 mg P/L and was prepared using tap water and reagent-

**Table 1** Iron and steel slag samples from the Chicago-Gary area of Indiana and Illinois. Latitude and longitude are given in degrees, minutes, and seconds for legacy sites. Abbr. Basic Oxygen Furnace (BOF)

Sample	Site	Location	Size fraction	Furnace
ILSS1	legacy	41°41'12.05"N 87°33'57.82"W	crushed < 9.5 mm	unknown
ILSS2	legacy	41°39'44.46"N 87°32'38.04"W	C-fines, < 9.5 mm	unknown
ILSS5	legacy	41°45'06.95"N 87°32'33.97"W	crushed < 9.5 mm	unknown
ILSS6	legacy	41°39'41.00"N 87°29'45.20"W	crushed < 9.5 mm	unknown
ILSS7	legacy	41°39'44.93"N 87°30'59.82"W	crushed < 9.5 mm	unknown
ILSS8	legacy	41°39'02.02"N 87°31'22.66"W	crushed < 9.5 mm	unknown
AMFeC	modern	Arcelor Mittal Indiana Harbor	C-fines, < 9.5 mm	blast
AMSteelC	modern	Arcelor Mittal Indiana Harbor	C-fines, < 9.5 mm	steel (BOF)
USSFear	modern	U.S. Steel Corp. Gary Works	25-75 mm (1-3")	blast
USSFegan	modern	U.S. Steel Corp. Gary Works	0.075 – 4.7 mm (0.003-3/16")	blast
USSSteelB_3/8	modern	U.S. Steel Corp. Gary Works	9.5 mm (3/8")	steel (BOF)
USSSteelB_3/8-4	modern	U.S. Steel Corp. Gary Works	9.5 – 100 mm (3/8-4")	steel (BOF)
USSSteelC	modern	U.S. Steel Corp. Gary Works	C-fines,< 9.5 mm	steel (BOF)

grade  $\text{KH}_2\text{PO}_4$ . Columns were slowly saturated from the bottom to the top and then flow adjusted to reach a void hydraulic retention time of approximately 8 hours. Effluent was collected in pore volume increments and pH was measured hourly using an air-tight flow

through cell before effluent was exposed to the atmosphere (“initial pH”). The “final pH” of the pore volume, after exposure to the atmosphere, was as much as 1 pH unit lower than the initial pH because as the effluent equilibrated with CO<sub>2</sub> in the atmosphere, calcite precipitated, generating hydrogen ions and resulting in a lower pH.

Reacted solutions from experiments were filtered (0.45 μm) and analyzed by inductively coupled plasma-atomic emission spectrometry, inductively coupled plasma-mass spectrometry, and ion chromatography for major and trace elements. Phosphate was measured by spectrophotometry using the ascorbic acid method and alkalinity by titration. Geochemical modeling was performed using PHREEQC v. 3.3 and the minteq.v4 database.

## Results and Discussion

### Mineralogy and Chemistry

Modern and legacy slags (n = 13) generally have comparable chemical compositions with 10 – 44 wt. % CaO, 0.3 – 28 wt. % FeO, 10 – 44 wt. % SiO<sub>2</sub>, 1 – 15 wt. % Al<sub>2</sub>O<sub>3</sub>, 2 – 11 wt. % MgO, and 0.3 – 9 wt. % MnO. Modern iron and steel slags generally have higher concentrations of Ca than legacy slag (fig. 1). Modern granulated and coarse air-cooled iron slags have the least amounts of Fe (1 wt. % FeO or less). Commonly identified mineral phases include: larnite, brownmillerite-srebrodolskite, melilite, wustite, spinel, calcite, quartz and cristobalite, and iron metal. The granulated iron slag is nearly all amorphous glass. Glass is less abundant, although likely present, in the other slag samples. The bulk chemistry and mineralogy of these samples are comparable to those reported for ferrous slag throughout the world (Piatak et al. 2015).

### Neutralization Potential

Most slags produce alkaline paste pH values (pH 10 – 13) and have high net neutralization potentials (NNP) (400 – 830 kg CaCO<sub>3</sub>/t). The highest NNP values are equivalent to approximately 80 % the neutralization potential of pure calcite or limestone (fig. 1). Samples with the highest NNP include modern iron granulated slag and the coarse-size fractions of modern, air-cooled iron and steel slags. Interestingly, two legacy samples offer comparable neutralization potentials to the modern materials (fig. 1). NNP correlates strongly with total Ca content (fig. 1). The Ca minerals in the slag (calcite, larnite, and rankinite) consume acid during hydrolysis, explaining this correlation. The slags with the highest NNP may be useful in treating acidic solutions such as acid-mine drainage from coal or base-metal operations as was reported by Simmons et al. (2002) who utilized ferrous slag as a filter in a leach bed that successfully neutralized acidic coal-mine drainage in West Virginia, USA.

### Phosphate Removal Capacity

Batch experiments demonstrate efficient removal of phosphate from solutions with initial phosphate concentrations ranging from 10 to 1,085 mg P/L. At the lowest tested phosphate concentration of 10 mg P/L, 12 of the 13 slags removed essentially all of the phosphate from the solution (98 – 100 % retained in solid), with the lowest removal of 98 % measured for the coarse air-cooled blast-furnace slag (USSFear), which had the lowest specific sur-

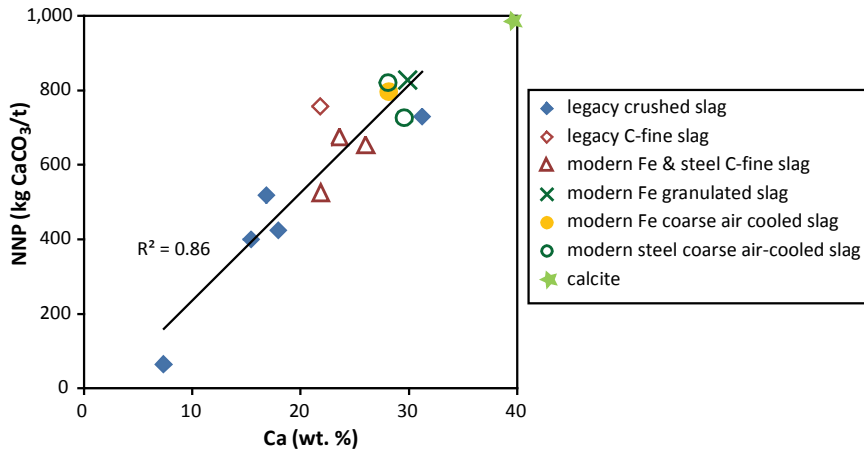


**Figure 1** Bulk calcium (Ca) concentrations in weight percent (wt. %) versus Net Neutralization Potential (NNP) of slag in kilograms CaCO<sub>3</sub> per ton (kg CaCO<sub>3</sub>/t). Theoretical calcium concentration and NNP for calcite are shown. The linear regression line for slag data and coefficient of determination (R<sup>2</sup>) are also indicated.

face area. The one exception, with removal of 75% P, was slag from a legacy site (ILSS8). This sample contains the lowest Ca concentration and the highest Al and Fe concentrations. Additionally, the mineralogy is unique with significant plagioclase feldspar and hematite, which are atypical primary phases in ferrous slag (Piatak et al. 2015); this sample may contain non-slag materials, in addition to being weathered.

Four slag samples and a limestone were tested in batch experiments using increasingly higher phosphate leachate concentrations (54, 108, 256, and 501 mg P/L). The following indicates the phosphate-removal effectiveness of the samples tested: AMSteelC and AMFeC > ILSS1 > limestone > ILSS2. The modern C-fines retained all of the phosphate in the 501 mg P/L solution. The final set of batch experiments using a 1,085 mg P/L leachate solution resulted in only partial removal of the phosphate for all tested samples. These results provided data for the determination of maximum phosphate removal capacities (PRC in mg P/g slag) of slag samples:

$$\text{PRC} = ((P_{\text{in}} - P_{\text{ef}})V)/M$$

where  $P_{\text{in}}$  is the initial phosphate concentration in mg P/L,  $P_{\text{ef}}$  is the effluent phosphate concentration (mg P/L),  $V$  is the volume of solution (L), and  $M$  is the mass of the slag (g). Overall, the most effective slags are two modern air-cooled C-fines (AMFeC and AMSteelC) with PRCs reaching 18 mg P/g of slag (fig. 2); this is the least marketable type of slag because the larger air-cooled fractions are generally preferred for use in construction materials (for example, ballast, riprap, gabion) and granulated glassy slag is sold for use in cement. Limestone was also effective with a PRC of 17 mg P/g of limestone. Several modern and legacy samples performed similarly and include: modern granulated iron (USSFegran), modern

air-cooled coarse and C-fine steel slag from the Gary Works location (USSSteelB\_3/8, USSSteelC), legacy C-fines (IILSS2), and legacy air-cooled (ILSS1), all with PRCs between 13–14 mg P/g of slag. Slightly less effective were air-cooled slag from several legacy sites (ILSS5, ILSS6, and ILSS7), with PRCs between 9–10 mg P/L, and the least effective was legacy air-cooled ILSS8 (PRC of 2 mg P/g of slag) (fig. 2).

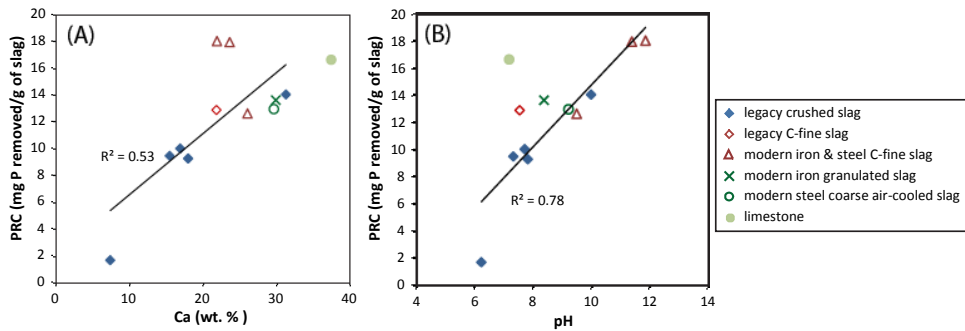


**Figure 2** Results from batch experiments using initial leachate phosphate concentration of 1,085 mg P/L. (A) Phosphate removal capacity (PRC) versus bulk calcium (Ca) concentrations in weight percent (wt. %). (B) PRC versus pH of reacted leachate solution. The linear regression line and coefficient of determination ( $R^2$ ) are also indicated.

White secondary coatings formed on reacted slag during batch tests. Based on XRD, the white coating regularly contained calcite and Ca phosphate phases, most commonly brushite ( $\text{CaHPO}_4 \cdot 2\text{H}_2\text{O}$ ), but also apatite phases such hydroxylapatite ( $\text{Ca}_5(\text{PO}_4)_3(\text{OH})$ ) and carbonate-hydroxylapatite ( $\text{Ca}_5(\text{PO}_4)_3(\text{CO}_3)(\text{OH})$ ), suggesting phosphate removal occurs by precipitation.

As shown in figure 2A, the PRC correlates ( $R^2=0.5$ ) with bulk Ca content, similar to the finding for NNP and bulk Ca concentrations (fig. 1). Interestingly, samples of C-fines from the Indiana Harbor location have substantially higher PRC than C-fines from Gary Works and legacy fines, despite having comparable bulk Ca contents (fig. 2A). Phosphate removal correlation with leachate pH is greater ( $R^2=0.8$ ) than observed for Ca content for slag samples, partially due to the C-fines placement in figure 2B. The pH of the effluent may be an indicator of the abundance of readily soluble Ca minerals that consume acid upon dissolution and increase pH. Slag that contains higher amounts of soluble Ca minerals results in a higher concentrations of dissolved Ca available to combine with the phosphate and precipitate. Calcite, also identified on reacted slag, influences pH by generating acid during precipitation. Secondary calcite formation may actually inhibit phosphate removal because it removes dissolved Ca from solution.

Preliminary data for ongoing flow-through experiments demonstrate that modern iron C-fine slag (AMFeC) has a higher phosphate removal capacity (PRC) and is effective over a longer period of time compared to composited crushed legacy slag from site ILSS5 (fig. 3A). The pH of the effluent from the modern C-fine column is higher than that from the legacy

materials due to differences in bulk chemistry and primary mineralogy (fig. 3B). Also, legacy slag is weathered, therefore, readily soluble Ca phases, some of which consume acid, may have been dissolved and washed away. As shown in figure 3C, the legacy slag initially retains nearly all the phosphate from the influent solution resulting in low effluent phosphate concentrations. However, after only approximately 5 pore volumes, the phosphate concentration in the effluent increases exponentially. Another slope change occurs after approximately 150 pore volumes, after which the phosphate concentrations increase in only small increments in the effluent. At 150 pore volumes, the legacy material is only retaining about 40 % of the influent phosphate. Calcium concentrations (fig. 3C) display a reverse trend to phosphate, generally decreasing exponentially then reaching a steadier value. Similar trends are observed for the modern slag for phosphate and Ca concentrations (fig. 3D). However, the modern material is effective at removing nearly all of the phosphate for a longer duration (over 200 pore volumes, compared to 5 pore volumes). Also, after the initial exponential increase in phosphate concentrations, the efficiency for phosphate removal leveled off to approximately 50 % phosphate retained at approximately 400 pore volumes, with only small increases after. These results suggest that the modern slag not only continues to remove phosphate longer, but also, more efficiently.

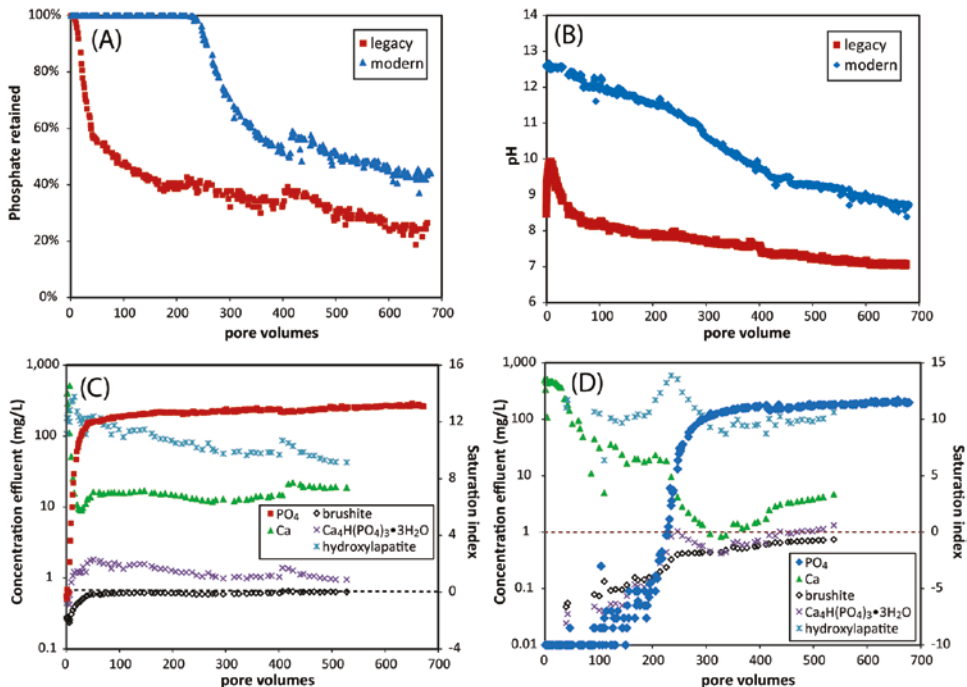


**Figure 3** Results from column experiments using modern slag (AMFeC) and legacy slag (ILSS5). (A) Percent phosphate ( $PO_4$ ) retained versus pore volume. (B) Initial pH of the effluent versus pore volume. Phosphate and calcium (Ca) concentrations in effluent and saturation indices for Ca-phosphate phase for legacy slag (C) and the modern slag (D). Horizontal dashed lines mark saturation indices of zero. Some results are not shown for all pore volumes because experiments and analyses are ongoing.

The dissolution of Ca silicates and oxides in the slag likely increases  $\text{Ca}^{2+}$  and  $\text{OH}^-$  concentrations, which reacts with phosphate to form Ca phosphates. Under acidic to near neutral pH, brushite ( $\text{CaHPO}_4 \cdot 2\text{H}_2\text{O}$ ) is predicted to form from aqueous solutions, whereas under alkaline conditions, octacalcium phosphate ( $\text{Ca}_8(\text{HPO}_4)_2(\text{PO}_4)_4 \cdot 5\text{H}_2\text{O}$ ) may form before converting into Ca-deficient hydroxylapatite ( $\text{Ca}_{10-x}(\text{HPO}_4)_x(\text{PO}_4)_{6-x}(\text{OH})_{2-x}$  ( $0 < x < 1$ )), which then may age to hydroxylapatite ( $\text{Ca}_5(\text{PO}_4)_3(\text{OH})$ ), which is stable and insoluble (Dorozhkin 2016). Amorphous Ca phosphate has also been found to form before crystalizing to more stable forms. Bowden et al. (2009) reported a sequence of Ca-phosphate phases on reacted steel slag in column experiments from the most soluble brushite to octacalcium phosphate and hydroxylapatite over time. Interestingly, the legacy slag in this study generates an effluent that, based on geochemical modeling, is oversaturated with respect to hydroxylapatite and octacalcium phosphate (represented in the geochemical database as  $\text{Ca}_4\text{H}(\text{PO}_4)_3 \cdot 3\text{H}_2\text{O}$ ) but after 40 pore volumes is approximately saturated with respect to brushite (saturation index  $\sim 0$ ) (fig. 3C). Brushite was identified by XRD in precipitate that formed in the effluent from this column, further supporting the hypothesis that precipitation of Ca phosphate is a main removal mechanism. Geochemical modeling of Ca-phosphate phases for the modern slag column effluents results in saturation indices that are oversaturated for hydroxylapatite; however brushite and octacalcium phosphate saturation indices approach zero after approximately 250 pore volumes (fig. 3D). The formation of octacalcium phosphate from more alkaline solutions reported by Dorozhkin (2016) may be consistent with its presence in the modern slag column with higher pH effluent. (Once the kinetic experiments are terminated, mineralogical identification of secondary precipitates formed within both columns will be conducted to compare to modeling results.) Some Ca phosphate phases such as brushite are more soluble at low and high pH (Dorozhkin 2016), therefore the higher pH conditions in the modern slag column compared to the legacy slag column (fig. 3B) may inhibit its initial precipitation. The mechanism that drives the phosphate removal previous to that requires further investigation. Precipitation of Fe phosphates may play a role. Also, calcite actively precipitated from effluent generated in the modern slag column for approximately the first 250 pore volumes, generally the same duration that brushite and octacalcium phosphate were undersaturated. During these initial pore volumes, primary Ca phases in the slag and secondary calcite may have provided sorption sites for phosphate. According to Bowden et al. (2009), absorbed phosphate on calcite may form nucleation sites from which precipitation of Ca phosphates may occur; however, limited sites are likely available on the calcite. Further, most of the secondary calcite began forming only after the effluent was exposed to atmospheric  $\text{CO}_2$ . Iron phases in the slag (iron metal, wustite) may also provide sorption sites. However, sorption of phosphate would likely be limited under these high pH conditions. Additionally, phases not in the geochemical database such as amorphous Ca phosphate or Ca-deficient hydroxylapatite may be controlling Ca and phosphate concentrations.

After the phosphate removal efficiency of both columns declines sharply, a much slower decline is observed and maintained for many pore volumes. Initially, the dissolution of the more soluble Ca-bearing minerals provides readily available Ca to combine with the phos-



phate. The sharp decline may occur once the readily soluble Ca is exhausted and/or armoring by precipitates occurs on slag grains. Subsequently, the influent solutions become a significant source of Ca ions available for Ca-phosphate precipitation. Modeling indicates that the influent solution used is supersaturated with respect to brushite, and white precipitates appeared to continue to accumulate in the column. Slag dissolution facilitated the initial nucleation of phosphate precipitation, which continues to occur due to a continuous supply of Ca in the influent. This effect was also observed by Bowden et al. (2009). This has interesting implications for water treatment scenarios such that phosphate removal may continue past predictions based on a slag's PRC if the water to be treated is a source of Ca ions to the system. However, the precipitation of calcite and Ca phosphate may eventually decrease the hydraulic conductivity and dispersivity in treatment systems. To date, the cumulative PRC of the columns are 12 mg P/g of slag for legacy ILSS5 and 15 mg P/g of slag for modern C-fines (AMFeC).

### Conclusions

Steelmaking slag may be a viable option for use in removing phosphate from municipal wastewaters or agricultural runoff or to treat acid solutions, such as acid-mine drainage. Because the bulk Ca content of the slags generally correlates with its effectiveness to remove phosphate and neutralize acid, determining Ca content maybe a useful initial assessment for identifying and ranking potential usable slag materials. Promoting the utilization of slag may reduce the amount disposed as waste at modern facilities, help offset restoration costs at legacy sites, and decrease the need to mine natural materials for water treatment applications.

### Acknowledgements

The authors thank Arcelor Mittal and U.S. Steel Corporation for providing modern steelmaking slags. Travis Cole and Robert Kay, of the U.S. Geological Survey, assisted in collecting slag samples at legacy sites. Jane Hammarstrom and Sarah Hayes, of the U.S. Geological Survey, provided helpful review comments that improved the text.

### References

- Bowden LI, Jarvis AP, Younger PL, Johnson KL (2009) Phosphorus removal from waste waters basic oxygen steel slag. *Environ Sci Technol* 43:2476-2481. doi:10.1021/es801626d
- Dorozhkin SV (2016) Calcium orthophosphates (CaPO<sub>4</sub>): occurrence and properties. *Prog Biomatter* 5(1):9-70. doi:10.1007/s40204-015-0045-z
- Piatak NM, Parsons MB, Seal RR II (2015) Characteristics and environmental aspects of slag: A review. *Appl Geochem* 57:236-266. doi:10.1016/j.apgeochem.2014.04.009
- Simmons J, Ziemkiewicz P, Black DC (2002) Use of steel slag leach beds for the treatment of acid mine drainage. *Mine Water Environ* 21:91-99. doi:10.1007/s102300200024